

LiAlD₄ with VCl₃ additives: Influence of ball-milling energies

D. Blanchard, A.I. Lem, S. Øvergaard, H.W. Brinks, B.C. Hauback*

Institute for Energy Technology, P.O. Box 40, NO-2027 Kjeller, Norway

Received 2 January 2007; received in revised form 29 March 2007; accepted 2 April 2007

Available online 6 April 2007

Abstract

The reduction reaction of VCl₃ mixed with LiAlD₄ is studied for different ball-mill energies. From low to high ball-milling energies VCl₃ is reduced by the formation of Li–V–Cl metastables phases, LiCl and free Al and V or Al–V phases. It is also shown that the enhancement of the kinetics reaches a limit with increased ball-mill energy. From measurements of the released hydrogen with a Sieverts apparatus and X-ray and neutron diffraction, it is shown that even under mild conditions, at or close to room temperature, the two first steps of the decomposition of VCl₃-enhanced LiAlD₄ occurs during the first weeks after milling at temperatures in the range 20–50 °C.

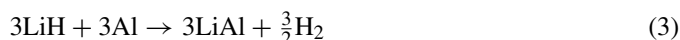
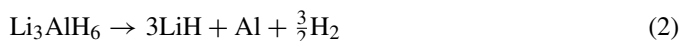
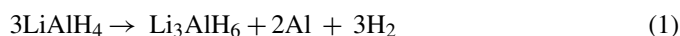
© 2007 Elsevier B.V. All rights reserved.

Keywords: Hydrogen-storage materials; Alanates; Metal hydrides; Ball-milling

1. Introduction

Since the work by Bogdanovic and Schwickardi [1] showing the improved kinetics and reversibility of Ti-enhanced NaAlH₄ at moderate conditions, alanates mixed with transition metal additives have been widely studied for their possible utilization in onboard hydrogen-storage systems. Initially, wet chemistry methods were used to mix the alanate and the additives (e.g. in [1]) with the disadvantages of contamination and loss of weight capacities because of the use of solvent. Subsequently, dry ball-milling was used to add the transition metals [2], and this is now the preferential method. However, it is difficult to control the process because of the difficulties to accurately define the energy and the physical parameters during the milling.

The dehydrogenation of LiAlH₄ upon heating is a three steps reaction [3]:



* Corresponding author at: Institute for Energy Technology, Physics Department, NO-2027 Kjeller, Norway. Tel.: +47 63 80 60 78; fax: +47 63 81 09 20.

E-mail address: bjorn.hauback@ife.no (B.C. Hauback).

The desorption temperatures, T_1 and T_2 from Eqs. (1) and (2), can be significantly decreased by ball-milling the alanate with additives like VCl₃ [4,5]. The decomposition of LiAlH₄ at room temperature is slow [6] but has been shown to be significantly improved by adding TiF₃ [7].

The aim of the present work is to study the effect of the ball-milling conditions on the reaction between LiAlD₄ and VCl₃ and how this influences the decomposition kinetics of the alanate.

2. Experimental

The compounds, LiAlD₄ (≥95% purity, containing ~0.2 mol% LiCl) and VCl₃ (99.99%) were purchased from Sigma–Aldrich Corp. LiAlD₄ was used in this study instead of LiAlH₄ because it is commercially available with a higher purity. The samples were handled and stored in a glove box with a dry argon atmosphere to prevent any contact with oxygen or moisture.

Two different planetary Fritsch ball-mills (BM) were used. The Pulverisette 7 (P7) was equipped with hardened steel vials of 12 cm³ sealed under argon with three (Ø 12 mm, 7 g) or five steel balls (Ø 10 mm, 4 g). Typically 1 g samples were used, the ball to powder ratio (BPR) was ~20:1. Two different gyration rates were used, 510 and 720 rpm, respectively. The Pulverisette 6 (P6), with a 270 cm³ hardened steel vial equipped with a Gas pressure and Temperature Measuring system (GTM), allows recording pressure and temperature changes in the vial during the milling. For P6 50 steel balls (Ø 10 mm, 4 g) were used, and for a 1 g sample the BPR is 200:1. The gyration rate was 400 rpm and the temperature inside the vial increased by less than 10 °C during the milling time. The temperature measured in the P6 vials is the average temperature of the whole system including the vial, the balls, the powder and the gas. The increase in temperature during the milling results from the heat produced by the impact of the balls and does not reflect the temperature at the impact point of the balls. This latter cannot easily be detected and is obviously higher than the measured

temperatures. Nevertheless, no thermal decomposition of LiAlD_4 into Li_3AlD_6 and Al was measured after the ball-milling processes (see below).

Based on the expressions developed in [8] the estimated comparisons between the energies transferred to the powder with the BM P6 and P7 are $E_{P6} \approx 20E_{P7}$ for $\omega_{P7} = 720$ rpm and $\omega_{P6} = 400$ rpm, respectively, and $E_{P6} \approx 50E_{P7}$ for $\omega_{P7} = 510$ rpm and $\omega_{P6} = 400$ rpm. Thus, $E_{P6} \gg 50E_{P7}$, and the terminology low and high-energy BM will be used hereafter for milling with P7 and P6, respectively.

Constant temperature decomposition measurements (CTD) were carried out with a Sieverts apparatus. The sample holder with a pressure sensor from Presens AS (relative accuracy 1%) was placed inside a heating chamber with a temperature stability of ± 0.02 °C. The total volume of the setup was 10.995 cm^3 . 0.6 g samples were used with a typical pressure increase of maximum 30 bar.

Thermal Desorption Spectroscopy experiments (TDS) were carried out in dynamic vacuum at a constant heating rate of 2 °C/min. The vacuum level with empty sample holder was approximately 2×10^{-6} mbar. A Pt thermocouple placed inside the powder continuously recorded the temperature of the sample.

Powder X-ray diffraction data (PXD) were collected with a Bragg Brentano geometry INEL MPD diffractometer with Cu $K\alpha_1$ radiation and a curved 120° position sensitive detector. The powder was uniformly spread as a thin layer in the sample holder, and covered by a thin polyethylene film (PE) to prevent contact with oxygen or moisture during the measurements. A small diffuse scattering halo due to the PE film is visible at around 24° in 2θ in the diffractions patterns.

High-resolution synchrotron radiation powder diffraction data (SR-PXD) were measured at the Swiss-Norwegian beam line (SNBL) at station BM01B at the European Synchrotron Radiation Facility (ESRF) in Grenoble, France. The samples were kept in rotating 0.8 mm glass capillaries. The wavelength 0.49956 \AA was obtained from a channel-cut Si (1 1 1) monochromator.

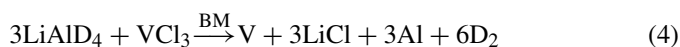
Powder neutron diffraction (PND) in situ data were collected between $2\theta = 10^\circ$ and 130° with the PUS instrument at the JEEP II reactor at Kjeller, Norway [9]. The data were rebinned in steps of $\Delta(2\theta) = 0.05^\circ$. Neutrons with wavelength 1.5554 \AA were obtained from a focusing Ge(5 1 1) monochromator. The sample was kept in a quartz tube ($\varnothing 6 \text{ mm}$) connected to a vacuum pump. A water-cooled furnace placed around the sample was used to heat the sample. The sample was kept at 40 and 50 °C for 6 h, and then cooled to 18 °C for the PND measurements.

Rietveld refinements of the diffraction patterns were carried out using Rietica [10] and Fullprof [11] softwares. Structural data for LiAlD_4 and Li_3AlD_6 were taken from [12] and [13], respectively. In Rietica, Voigt profile functions were used and the background was modeled by Chebyshev II polynomials. Pseudo-Voigt functions and interpolation between manually selected background points were used in Fullprof.

3. Results and discussion

3.1. Reactions during ball-milling

High-energy BM using P6 were carried out for LiAlD_4 mixed with 5, 10 and 25 mol% VCl_3 , respectively. The pressure and the temperature within the vial were recorded during the milling. Fig. 1 shows the quantity $n_{D_2}/6n_{VCl_3}$ versus the time t for the three samples. This quantity should be equal to one if the reduction of VCl_3 is complete and follows the reaction:



The pressure in the vial was monitored during the milling process. The milling times were chosen in order to achieve a complete reduction of VCl_3 and to avoid possible thermal decomposition of LiAlD_4 that may occur with longer milling times.

n_{D_2} , the number of moles of deuterium formed during the milling, is calculated from the pressure and temperature measurements using the equation of state. n_{VCl_3} is the number

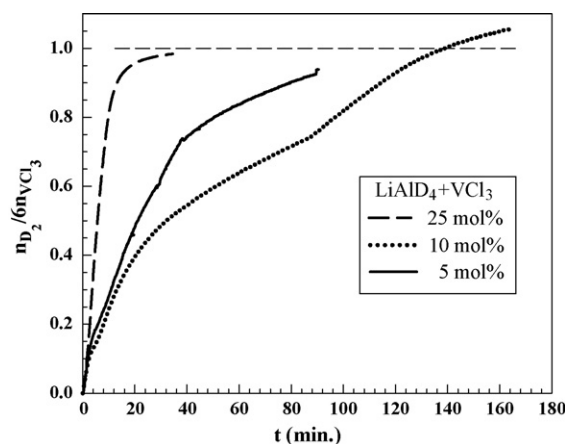


Fig. 1. The evolution of $n_{D_2}/6n_{VCl_3}$ as a function of time for BM LiAlD_4 with 5, 10 and 25 mol% VCl_3 .

of moles of VCl_3 introduced in the vial. For all experiments $n_{D_2}/6n_{VCl_3}$ approach values close to 1, in agreement with Eq. (4). The final value is slightly higher ~ 1.035 for the 10 mol% VCl_3 sample. This deviation may result from experimental errors or from the thermal decomposition of a fraction of LiAlD_4 into Li_3AlD_6 , and Al. However, this decomposition must be very small since Li_3AlD_6 was not found in the PXD pattern (see below).

A stoichiometric mixture of LiAlD_4 with 25 mol% VCl_3 gave $n_{D_2}/6n_{VCl_3} > 0.98$ after 32 min of milling. In that case LiCl is the only well-crystallized phase seen by PXD (Fig. 2a). A broad peak, with its maximum at approximately $2\theta = 41^\circ$ and covering 10° in 2θ , is also present in the diffraction pattern. After annealing the powder for 16 h at 400 °C under vacuum, the broad peak is no longer present, and new well-defined peaks from Al_3V are observed in the PXD data (Fig. 2b). The phase composition of the annealed sample was calculated by quantitative phase analysis (QPA) to be 22 mol% Al_3V and 78 mol% LiCl . This is close to the theoretical values of 25 and 75 mol%, respectively. Solid-solution of Al(V) and V(Al) as well as some metastable Al–V phases have been observed in a ball-milled 75% Al–25%

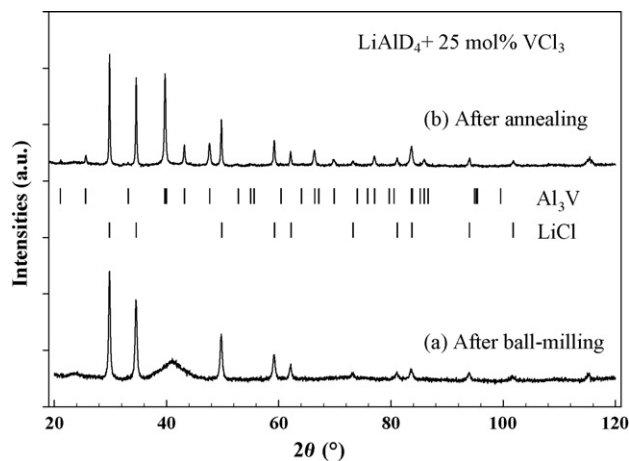


Fig. 2. PXD patterns of LiAlD_4 with 25 mol% VCl_3 . (a) After BM. The position of the Bragg peaks for LiCl and Al_3V are shown. (b) After BM and annealing at 400 °C for 15 h.

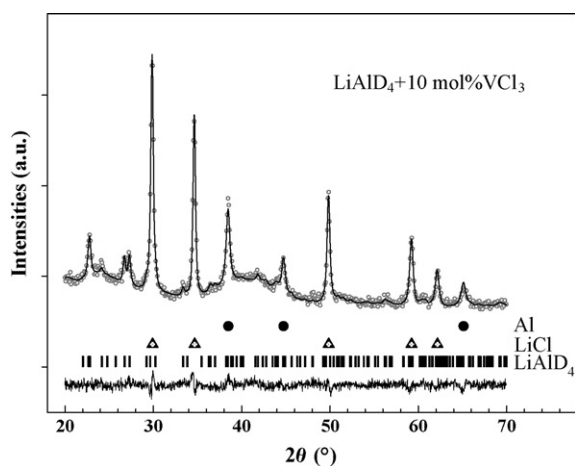


Fig. 3. PXD pattern of LiAlD_4 with 10 mol% VCl_3 after BM for 164 min showing observed (circles), calculated (from Rietveld refinement) (upper line) and difference (bottom line) plots. The positions for (from top): Al, LiCl and LiAlD_4 are shown in the plot.

V mixture [14]. These phases have their main reflection peak at about $d = 2.2 \text{ \AA}$, corresponding to $2\theta = 41^\circ$ with Cu $K\alpha$ radiation. When doubling or tripling the milling times of this mixture, Al_3V was formed [14]. Thus, the broad peak observed in the fresh milled powder can be interpreted as nanocrystalline Al–V phases.

LiAlD_4 with 10 mol% VCl_3 was BM for 164 min. The D_2 evolution is shown in Fig. 1. PXD of the fresh sample (Fig. 3) shows the presence of LiAlD_4 , Al and LiCl, but no VCl_3 or Li_3AlD_6 . The same broad peak observed in the stoichiometric (25 mol% VCl_3) BM mixture and interpreted as a nanocrystalline Al–V phase is also present in the 10 mol% VCl_3 sample at around $2\theta = 41^\circ$ with a span of 10° . This broad peak was considered to be part of the background during the Rietveld refinements.

BM of LiAlD_4 with 5 mol% VCl_3 was performed for 5, 20 and 90 min, respectively (samples A, B and C). PXD diagrams measured immediately after BM are shown in Fig. 4. For sample A, only a weak broad peak at around 14.7° (not shown in Fig. 4a) confirms the presence of remaining VCl_3 in the sample (corresponding to the most intense (003) reflection for VCl_3). For samples B and C no other crystalline phases than LiAlD_4 , Al and LiCl are observed.

The phase compositions calculated from QPA of the PXD data and from the pressure in the vial at the end of the ball-

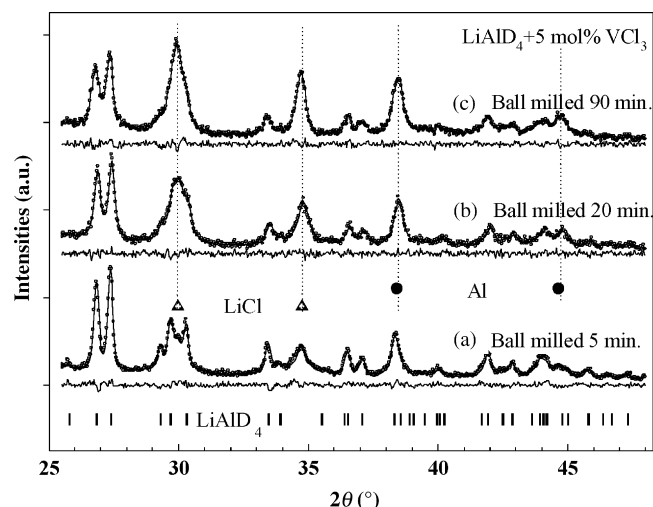


Fig. 4. PXD patterns of LiAlD_4 with 5 mol% VCl_3 after BM for (a) sample A: 5 min. (b) Sample B: 20 min and (c) sample C: 90 min. Observed (circles), calculated (from Rietveld refinements) (upper line) and difference (bottom line) plots are shown.

milling, respectively, assuming that only the reduction reaction in Eq. (4) occurs, are shown in Table 1 for the LiAlD_4 samples with 5 and 10 mol% VCl_3 . For the 10 mol% sample the Al:LiCl ratio from QPA is significantly less than one, which may be caused by the formation of Al–V phases. For sample A the phase compositions determined from pressure measurement and Rietveld refinements differ slightly, but for samples B and C the agreements are very good. Nevertheless, the results obtained from the PXD refinements give systematically a slightly higher amount of LiCl and a slightly smaller amount of Al compared to the amounts calculated from n_{D_2} . Similar to the 10 mol% sample, the discrepancy may arise from some non-detectable small quantities of the Al–V phases, despite no broad peaks are visible in the diffraction patterns (Fig. 4).

The ratio Al:LiCl decreases by increased BM duration and amount of VCl_3 . A ratio less than one indicates that some of the Al is not present as free Al (as expected from Eq. (4)). The results for the samples with 25 and 10 mol% VCl_3 show that the missing Al has formed Al–V phases. Prolonged milling times and a higher VCl_3 content may result in better contacts between Al and V in favorable conditions, and thereby form Al–V phases.

Low energy BM of LiAlD_4 with 8 mol% VCl_3 was performed for 20 min at 510 rpm. SR-PXD measurement was carried out

Table 1

Phase compositions calculated from the pressure measurements in the BM vial and quantitative phase analysis of the Rietveld refinements of the PXD patterns for VCl_3 -enhanced LiAlD_4 with different mol fractions and ball-milling times

Samples	$n_{D_2}/6n_{\text{VCl}_3}$	Phase composition					
		From BM pressure			From PXD		
		LiAlD_4	Al	LiCl	LiAlD_4	Al	LiCl
10 mol% VCl_3 BM164 min	1.035	53.6	23.2	23.2	57.4	16.3	26.3
(A) 5 mol% VCl_3 BM 5 min	0.185	94.5	2.7	2.7	90.0	5.7	4.3
(B) 5 mol% VCl_3 BM 20 min	0.475	86.4	6.7	6.7	86.0	6.4	7.6
(C) 5 mol% VCl_3 BM 90 min	0.925	76	12	12	76.0	10.4	13.6

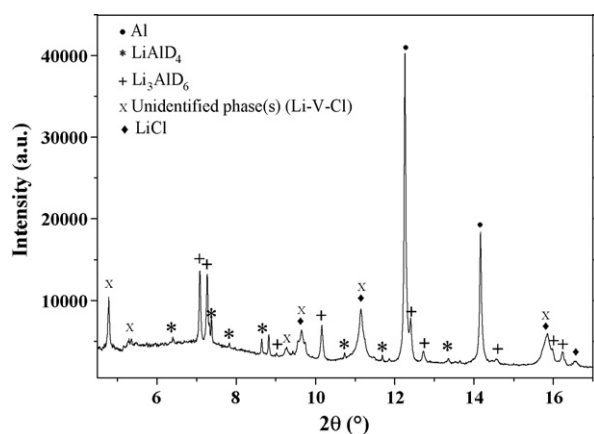


Fig. 5. SR-PXD pattern of LiAlD₄ with 8 mol% VCl₃ BM for 20 min. The data are collected after 16 days of storage at room temperature.

after 16 days of storage at room temperature (Fig. 5). LiAlD₄, Li₃AlD₆ and Al are clearly identified in the diagram. Under storage at room temperature LiAlD₄ decomposes according to Eq. (1) (see next paragraph). VCl₃ is not observed in the data, but some un-indexed reflections are present. These reflections, denoted by X in Fig. 5, overlap with some of the LiCl peaks. For pure LiCl the intensity of the (1 1 1) reflection at $2\theta = 9.7^\circ$ should be higher than the intensity of the (2 0 0) reflection at $2\theta = 11.2^\circ$. The opposite is observed in Fig. 5 indicating that at least one additional phase contributes to the SR-PXD data.

Two well-described cubic Li–V–Cl phases: Li₂VCl₄ [15] and Li_{1.3}V_{1.2}Cl₄ [16], give diffraction peaks close to the observed extra reflections. However, some of the X peaks are slightly out of position compared to the simulated patterns for these cubic phases indicating a lower symmetry (e.g. tetragonal). The phase diagram for the system LiCl–VCl₂ was studied by Hanebali et al. [17]. They reported the existence of a solid-solution of Li⁺ in VCl₂ for $75 \leq \tau \leq 96\%$, giving phases of the general formula Li_zV_{1-z/2}Cl₂. τ is the molar percentage of VCl₂ in the initial mixture of LiCl–VCl₂. These phases have a hexagonal structure with a slight elongation of the *c* axis compared to the cubic structure. The elongation tends to disappear when *z* increases. Le Bail refinement of our data, with a hexagonal structure for the unknown phase gave a satisfactory fit. However, better data and a single-phase sample are needed to completely index and solve the structure of the Li–V–Cl phase(s). Nevertheless, the phase(s) seem to have a composition close to LiVCl₃. They are probably metastable mixed valence compounds formed from non-stoichiometric amounts of Li, V and Cl.

Under storage at room temperature, the amount of VCl₃ that has not reacted during the milling process disappears and the fraction of Li–V–Cl phases increases. With no remaining VCl₃ in the sample, the amount of Li–V–Cl phase decreases while the LiCl content increases. Thus, the Li–V–Cl phases seem to be metastable phases with respect to LiCl, D₂ and Al + V or Al–V, but stable with respect to LiAlD₄ + VCl₃.

By lowering the milling energy, the redox reaction (Eq. (4)) may then proceed through intermediate metastable Li–V–Cl phases (LiVCl₃ is used to illustrate the reaction) that are not

detectable when higher milling energy are used:



It is clear that variations in the BM parameters are of critical importance for the reactions taking place and the products obtained from the milling process. The input energy during the milling determines the final state of V; ranging from un-reacted VCl₃ or the formation of intermediate metastable phases at low energies to the complete reduction of V when high-energy BM is applied. Furthermore, variations in the energies, the milling times or the molar ratios of the reactants lead to free Al and/or an Al–V phase.

In spite of the significant efforts to understand the solid-state reaction in the alanate system, the role of the additives is still unsatisfactory explained and understood. For NaAlH₄ mixed with Ti-based additives, studies have shown evidences on the presence of an amorphous or poorly crystallized Al–Ti alloy directly after ball-milling while upon cycling an Al_{1-x}Ti_x solid solution is formed [18–20]. For stoichiometric mixtures of titanium halides and LiAlH₄, Al–Ti alloys are formed directly after BM [21,22]. Herein, we have shown that Al–V phases are formed. The role of these binary phases, as amorphous or as solid-solution compounds, has not yet been identified and it is not known if they contribute to the observed enhanced kinetics of decomposition. In any case, the milling conditions should be adapted to promote or avoid the formation of these phases while ensuring a complete reduction of the additives.

3.2. Effect of the ball-milling energy on the stability of LiAlD₄ ball-milled with VCl₃

In order to determine the role of the milling energy, the stability of LiAlD₄ BM with 2 mol% VCl₃ under different conditions, was investigated by PXD and TDS during storage at room temperature. Table 2 gives a detailed list of the P7 parameters for the six samples (#1–6).

TDS was performed for the fresh samples, and the decomposition temperatures, *T*₁ and *T*₂, are given in Table 2. A typical TDS curve is shown in Fig. 6. The relative BM energies are calculated according to [8] with *E*₀, the energy transferred to the powder for sample 1, defined as the reference energy. When the decomposition temperatures are plotted as a function of BM energy, see Fig. 7, it is clear that *T*₁ is decreased by increasing BM energy, but reaches a lower constant level at approximately 3–4*E*₀. *T*₂ is lowered by BM, but appears to be independent of the milling energy. Similar results have been found for BM lithium alanate (without additives) [23], and NaAlH₄ ball-milled with TiCl₃ [24]. The decomposition temperature *T*₁ is lower, and thus Li₃AlD₆ is present at lower temperatures in VCl₃-enhanced LiAlD₄. This may result in a decomposition of Li₃AlD₆ at lower temperatures.

PXD patterns of the samples stored at room temperature were collected at regular time intervals; the first was measured immediately after the sample preparation. The molar fraction compositions of the samples were obtained from QPA based on Rietveld refinements. The possible presence of Li–V–Cl phases

Table 2
Milling parameters for the preparation for samples 1–6 of LiAlD₄ with 2 mol% VCl₃

Sample #	Time (min)	ω (rpm)	Balls #	Wt/ball (g)	T_1 (°C)	T_2 (°C)	k at RT	p
1	5	510	3	7	153	197	0.15×10^{-2}	0.6
2	5	720	3	7	123	202	1.92×10^{-2}	0.76
3	20	510	3	7	–	–	4.91×10^{-2}	0.82
4	20	510	3	7	–	–	4.86×10^{-2} (5.1×10^{-2})	0.82 (0.80)
5	40	510	3	7	107	190	7.86×10^{-2}	0.94
6	20	720	5	4	110	193	10.25×10^{-2}	0.92

All samples except sample 3 were pre-milled (without additives) at $\omega = 370$ rpm for 30 min in P7. The temperatures were obtained from TDS measurements (heating rates 2 °C/min). T_1 and T_2 are the temperatures for decomposition based on Eqs. (1) and (2), respectively. The rates of decomposition at room temperature (k) and the exponents (p) are determined from the JMA plots (Fig. 8). For sample 4 the value in parenthesis for k and p were calculated from the PND measurements.

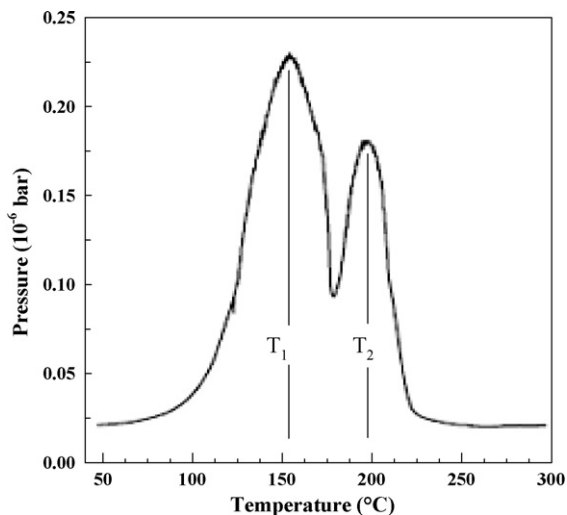


Fig. 6. TDS of sample 2 after 7 days of storage at room temperature. Heating rate 2 °C/min from room temperature up to 300 °C. $T_1 = 153$ °C and $T_2 = 197$ °C are the temperatures for the two decomposition reactions, Eqs. (1) and (2), respectively.

was ignored because of the small amount of VCl₃ (2 mol%). As an example, typical plots for the evolution of the mol fractions of the considered phases for sample 4 are shown in Fig. 8. Note that after reaching a maximum (after about 30 days of stor-

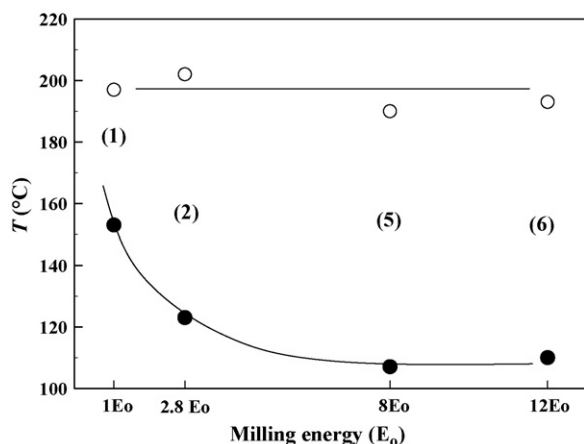


Fig. 7. Temperatures of decomposition (T_1 : ● and T_2 : ○), obtained from TDS experiments, vs. the energy transferred to the powder during the milling process. E_0 is the energy transferred to sample 1 and taken as a reference. The sample numbers are given in the figure. The lines have been drawn to show the trend of the data.

age), the amount of Li₃AlD₆ starts to decrease showing that the hexahydride phase also decomposes at room temperature. The decomposition of Li₃AlD₆ at room temperature occurs for all samples except for sample 1.

The decomposition of LiAlD₄ is a solid-state reaction. The John-Mehl Avrami formalism (JMA) [25] was used to calculate the rate of the first decomposition step (Eq. (1)). The volume fraction of LiAlD₄ (φ) in the sample at a time t can be expressed as:

$$\varphi = e^{-(kt)^p} \quad (6)$$

where k is the rate of the first step decomposition (Eq. (1)).

Fig. 9 shows the evolution of the volume fraction of LiAlD₄ as a function of time t for samples 1–6 stored at room temperature. The plot of the double logarithm of Eq. (6) gives a straight line. k and p are determined by least-square methods for the six samples, and give an acceptable agreement to the experimental data, as shown by the solid lines in Fig. 9. The values for k and p are given in Table 2. The value of p can be used to characterize the nucleation and growth processes of the new phases occurring during the solid-state decomposition [26,27]. The LiAlD₄ decomposition has recently been studied with this formalism [28]. The present values of p between 0.6 and 0.9 are consistent with values found in [28]. However, the temperature dependence should be noted.

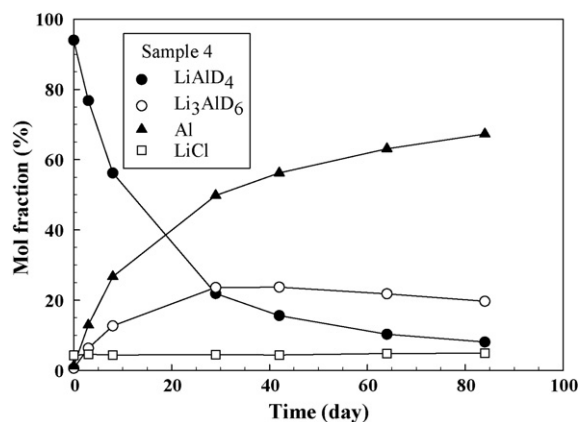


Fig. 8. Evolution of LiAlD₄, Li₃AlD₆, Al and LiCl molar fractions during storage at room temperature of sample 4 from QPA of the PXD data (from Rietveld refinements).

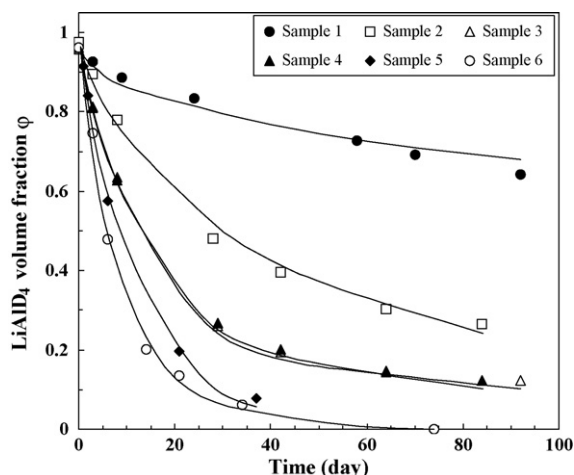


Fig. 9. Evolution of the volume fraction of LiAlD₄ in samples 1–6 stored at room temperature from QPA of the PXD (Rietveld refinements). The curves are plotted using Eq. (6) with k and p parameters calculated from the JMA plots.

The k -values for the six samples are plotted as a function of the energy transferred to the powder during the milling process in Fig. 10 ($1E_0$ is defined as the reference for sample 1, see above). The figure shows that the rate of decomposition at room temperature (k) increases with increasing BM energy. The accuracy of this method is illustrated by the similar k -values for the equally prepared samples 3 and 4. From the form of the curve (presented to show the trend) the decomposition seems to reach a certain maximum limit that is not obtained in these experiments. This trend is similar to the limit reached for T_1 (as illustrated in Fig. 7).

From these TDS and PXD experiments, it is clear that, up to a certain limit, increased BM energy decreases the decomposition temperature and enhances the rate of the first step decomposition. Thus, the milling energy should always be adjusted in order to obtain the best kinetics of decomposition.

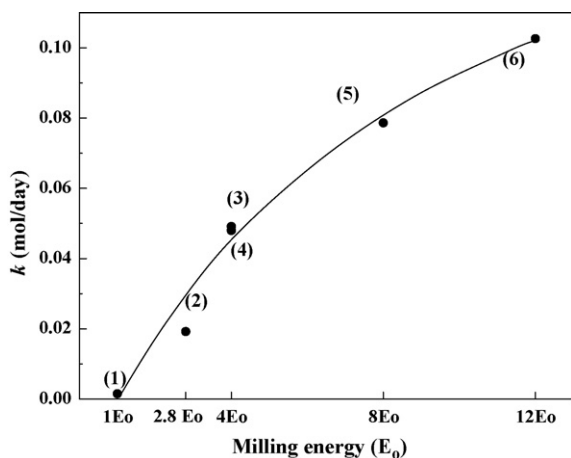


Fig. 10. k -Values (from the JMA plots) vs. the energy transferred to the powder during the milling process. E_0 is the energy given to the sample 1 and taken as a reference. The line has been drawn as a guide for the eye.

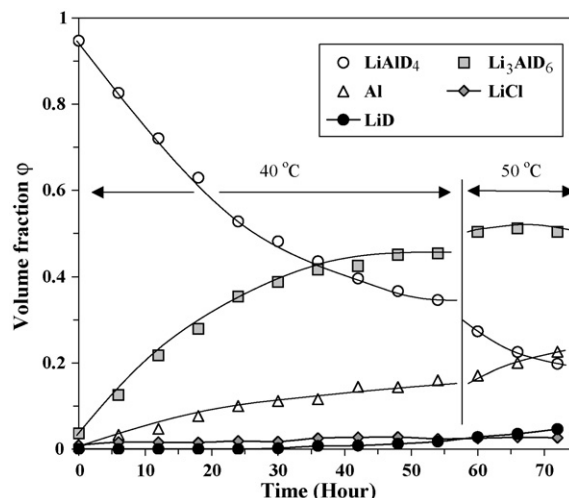


Fig. 11. Evolution of the volume fraction for LiAlD₄, Li₃AlD₆, Al, LiD and LiCl calculated from QPA (Rietveld refinement) of the PND patterns for sample 4. The first point is immediately after sample preparation (measured at 15 °C, the following nine points are for the sample kept at 40 °C for 6 h, and then at 50 °C for 6 h for the last three points. The PND data sets 2–13 were measured at 18 °C. The lines have been drawn as a guide for the eye.

3.3. Stability of LiAlD₄ ball-milled with VCl₃

The stability of LiAlH₄ stored at room temperature has previously been studied. For non-purified LiAlH₄, the hydrogen content was found to be reduced to 50% after 26 years of storage [6] while a purified sample was almost totally decomposed into LiAl after 9 years [29]. In our study, we have used LiAlD₄ instead of LiAlH₄. Despite it has been shown that isotopic substitution of deuterium for hydrogen leads to a more stable structure, LiAlD₄ should also decompose spontaneously at room temperature [30].

Herein, it has been found that BM VCl₃-enhanced LiAlD₄ decomposes rather quickly when stored at room temperature. In sample 6 LiAlD₄ is totally decomposed (according to Eq. (1)) after 75 days of storage. It is also found that Li₃AlD₆ starts to decompose after a relatively short time at mild conditions (storage at room temperature). Due to the poor X-ray scattering power of Li and D and the nearly equal unit cell dimensions for Al and LiD, it is difficult to distinguish between Al and LiD and detect LiD in the PXD patterns. Therefore, it is nearly impossible to use PXD to confirm the formation of LiD and thereby that the second reaction (Eq. (2)) takes place under the present experimental conditions. PND measurements were performed to clarify the presence of LiD.

The decomposition of sample 4 at 40 and 50 °C, was monitored by PND. A PND pattern at 15 °C was collected immediately after the sample preparation. For each of the following PND data sets the sample was first heated to 40 °C/50 °C and kept at the elevated temperature for 6 h. In order to reduce decomposition during the PND measurements to a minimum (each measurement takes 12 h), the PND data were collected at 18 °C. Nine patterns were measured after heating the sample to 40 °C and the following three patterns after heating the sample to 50 °C. The molar fraction composition of the sample was obtained from QPA with the LiAlD₄, Li₃AlD₆, Al, LiCl and

LiD phases. Fig. 11 shows the evolution of the fractions of the different phases for the 13 PND data sets as a function of the time the sample was kept at 40 and 50 °C. The JMA parameters are given in Table 2 and are in good agreement with the results from the PXD measurements. The curves exhibit the expected exponential decays and growths. Surprisingly, LiD starts to form after only 36 h of decomposition at 40 °C. At this stage the molar fraction of Li_3AlD_6 is still increasing due to the first decomposition step (Eq. (1)) even though the second decomposition step (Eq. (2)) is concurrently occurring. The three last measurements (after heating to 50 °C) clearly show the overlap of the two reactions and for the last measurement the amount of Li_3AlD_6 starts to decrease.

4. Conclusions

In this study, the importance of the ball-mill energies have been illustrated for LiAlD_4 with VCl_3 additives. When adding additives to alanates, systematic studies should be carried out to adjust the BM parameters in order to get a complete reduction of the additives, to lower the temperatures and to improve the kinetics for the thermal decomposition. Even under mild milling conditions the two first steps of the decomposition of LiAlD_4 with VCl_3 additives occurs during the first weeks after milling when the sample is kept at 20–50 °C.

Acknowledgements

The authors would like to acknowledge the EC for the financial support through the project “Hydrogen Storage in Hydrides for Safe Energy Systems–HYSTORY” (contract no. ENK6-CT-2002-00600) under the FP5 Energy Program. The skilful assistance from the project team at the Swiss-Norwegian Beam Line, ESRF, is gratefully acknowledged.

References

- [1] B. Bogdanovic, M. Schwickardi, *J. Alloys Compd.* 253 (1997) 1.
- [2] C.M. Jensen, R. Zidan, N. Mariels, A. Hee, C. Hagen, *Int. J. Hydrogen Energy* 23 (1999) 119.
- [3] W. Garner, F. Haycock, *Proc. R. Soc., A* 211 (1952) 335.
- [4] D. Blanchard, H.W. Brinks, B.C. Hauback, P. Norby, *Mater. Sci. Eng. B* 108 (2004) 54.
- [5] D. Blanchard, H.W. Brinks, B.C. Hauback, P. Norby, J. Muller, *J. Alloys Compd.* 404–406 (2005) 743.
- [6] T.N. Dymova, D.P. Alexandrov, V.N. Kkonoplev, T.A. Silina, A.S. Sizareva, *Koord. Khim.* 20 (1994) 279.
- [7] H.W. Brinks, A. Fossdal, J.E. Fonnelløp, B.C. Hauback, *J. Alloys Compd.* 397 (2005) 291.
- [8] N. Burgio, A. Iasonna, M. Magini, S. Martelli, F. Padella, *Il Nuovo Cimento* 13D (4) (1991) 459.
- [9] B.C. Hauback, H. Fjellvåg, O. Steinsvoll, K. Johansson, O.T. Buset, J. Jørgensen, *J. Neutron Res.* 8 (2000) 215.
- [10] B. Hunter, *Int. Union Cryst., Newslett.* 20 (1998) 21.
- [11] J. Rodríguez-Carvajal, *Physica B* 192 (1993) 55.
- [12] B.C. Hauback, H.W. Brinks, H. Fellvåg, *J. Alloys Compd.* 346 (2002) 184.
- [13] H.W. Brinks, B.C. Hauback, *J. Alloys Compd.* 354 (2003) 143.
- [14] F. Cardellini, V. Contini, G. Mazzone, *Philos. Mag. A* 78 (5) (1998) 1021.
- [15] M. Partik, M. Scheinder, H.D. Lutz, *Zeit. Ann. All. Chem.* 620 (1994).
- [16] M. Partik, H.D. Lutz, *Mater. Res. Bull.* 32 (1997) 1073.
- [17] L. Hanebali, T. Machej, C. Cros, P. Hagenmuller, *Mater. Res. Bull.* 16 (1981) 887.
- [18] A.G. Haiduc, H.A. Stil, M.A. Schwarz, P. Paulus, J.J.C. Geerlings, *J. Alloys Compd.* 393 (2005) 252.
- [19] H.W. Brinks, C.M. Jensen, S.S. Srinivasan, B.C. Hauback, D. Blanchard, K. Murphy, *J. Alloys Compd.* 376 (2004) 215.
- [20] H.W. Brinks, B.C. Hauback, S.S. Srinivasan, C.M. Jensen, *J. Phys. Chem. B* 109 (2005) 15780.
- [21] J.A. Haber, J.L. Crane, W.E. Buhro, C.A. Frey, S.M.L. Sastry, J.J. Balbach, M.S. Conradi, *Adv. Mater.* 8 (2) (1996) 163.
- [22] V.P. Balema, J.W. Wiench, K.W. Dennis, M. Pruski, V.K. Pecharsky, *J. Alloys Compd.* 329 (2001) 108.
- [23] A. Andreassen, T. Vegge, A.S. Pedersen, *J. Solid State Chem.* 178 (2005) 3672.
- [24] P. Wang, X.D. Kang, H.M. Cheng, *J. Alloys Compd.* 421 (2005) 217.
- [25] J. Burke, *The Kinetics of Phase Transformations in Metals*, Pergamon Press, Oxford, 1965.
- [26] W.E. Brown, D. Dollimore, A.K. Galwey, *Comprehensive Chemicals Kinetics*, vol. 22, Elsevier Scientific Publishing Company, Amsterdam, 1980.
- [27] A.T.W. Kempen, F. Sommer, E.J. Mittemeijer, *J. Mater. Sci.* 37 (2002) 1321.
- [28] D. Blanchard, H.W. Brinks, B.C. Hauback, *J. Alloys Compd.* 416 (2006) 72.
- [29] N.N. Malt'seva, A.I. Golonova, *Zh. Priklad. Khim.* 73 (2000) 705.
- [30] T.J. Frankcombe, G.J. Kroes, *Chem. Phys. Rev. Lett.* 423 (2006) 102.